Available online at www.sciencedirect.com
SCIENCE DIRECT®
International Journal of Heat and Mass Transfer 49 (2006) 2124–2136
International Journal of HEAT and MASS TRANSFER
www.elsevier.com/locate/ijhmt

A foam melting model for lost foam casting of aluminum

D.A. Caulk *

Manufacturing Systems Research Laboratory, General Motors Research and Development Center, 30500 Mound Road, Warren, MI 48090-9055, United States

Received 22 April 2005; received in revised form 28 November 2005
Available online 28 February 2006

Abstract

In lost foam casting of aluminum the liquid metal normally decomposes the foam pattern by ablation. But sometimes polymer vapor bubbling through the liquid metal accumulates along an upward-facing flow front until it opens a finite gap between the liquid metal and the decomposing foam. This changes the foam decomposition mechanism along that front from direct ablation to melting. A mathematical model is formulated for heat conduction, convection, and radiation across the gap, coupled with the vaporization of the excess polymer liquid behind the metal front and the resulting buoyant movement of polymer vapor bubbles through the liquid metal. Both models are combined to obtain an analytical solution for one-dimensional bottom filling of a pattern with uniform thickness. The results from this solution not only compare well with available experimental data, but they also explain how part thickness, metal temperature, and pressure affect filling speeds in bottom-fill situations.

Keywords: Lost foam casting; Gap; Melting; Foam decomposition; Model

1. Introduction

1.1. Lost foam casting

Lost foam casting is a relatively new foundry process that uses an expendable pattern made of molded polymer foam. The pattern is coated with a refractory material and placed inside a steel flask, where it is surrounded with loose, dry sand. After the sand is compacted by vibration, liquid metal is poured directly into the pattern, which decomposes ahead of the advancing liquid metal as gas and liquid products from the receding foam diffuse through the porous coating and into the sand. The liquid metal eventually replaces all the volume occupied by the foam pattern before it solidifies [1].

One of the important technical challenges in lost foam casting is to understand the connection between the mechanics of foam decomposition during mold filling and the formation of excessive internal porosity or folds (pairs of poorly fused metal surfaces contaminated by oxide and/or carbon residue) in the final cast product [2]. Such anomalies can occur when products of foam decomposition do not fully escape from the mold cavity before the casting solidifies. In a previous paper, Barone and Caulk [3] took an initial step towards understanding the mechanics of foam pattern decomposition by developing a model of foam *ablation* by the liquid metal, the dominant mechanism in lost foam casting of aluminum. But this mechanism, called *contact mode*, is not the only one responsible for decomposing the foam as the mold fills. Under certain process conditions, a large quantity of gas can accumulate between the liquid metal and the receding foam and drastically alter the mechanics of foam decomposition.

1.2. Gap mode

In aluminum lost foam casting, the foam pattern decomposes into both liquid and gas byproducts [3]. The gas escapes from the mold cavity by diffusing through the coating. After that, the coating absorbs what it can of

* Tel.: +1 586 986 0453; fax: +1 586 986 0574.
E-mail address: david.a.caulk@gm.com

0017-9310/$ - see front matter © 2006 Elsevier Ltd. All rights reserved.
doi:10.1016/j.ijheatmasstransfer.2005.12.007

Nomenclature

a_B	radius of a vapor bubble, m
$a^{\alpha\beta}$	contravariant components of the metric tensor on the casting surface
$\mathbf{a}_\alpha$	covariant base vectors on the casting surface
$\mathbf{a}^\alpha$	contravariant base vectors on the casting surface
c_A	specific heat of the air in the gap, J/kg K
c_S	specific heat of the solid polymer in the foam, J/kg K
c_V	specific heat of the polymer vapor in the decomposition layer, J/kg K
d	pattern thickness, m
d_C	coating thickness, m
F	geometric view factor for radiation across the gap
g	acceleration of gravity, m/s^2
h_G	effective heat transfer coefficient across the gap, W/m^2 K
H	liquid metal head at metal surface, m
H_M	latent heat of fusion per unit mass for the polymer in the foam, J/kg
k_G	thermal conductivity of the gas in the gap, W/m K
$\mathbf{k}$	vertically directed unit base vector
l_G	thickness of the gap, m
m	magnitude of the bubble flux vector, kg/m s
m_A	mass flux of air from the receding foam, kg/m^2 s
m_C	mass flux of polymer vapor lost from bubble flux by diffusion through the coating, kg/m^2 s
m_V	mass flux of polymer vapor into the gap from below, kg/m^2 s
$\mathbf{m}$	bubble flux vector, kg/m s
M_V	mass-average molecular weight of the polymer vapor in the gap, kg/mole
p_0	atmospheric pressure, Pa
p_M	pressure in the liquid metal, Pa
p_S	pressure on the outside surface of the coating, Pa
q	conduction heat flux across the gap, W/m^2
q_M	heat flux from the surface of the liquid metal into the gap, W/m^2
q_R	radiation heat flux from the liquid metal absorbed by the receding foam, W/m^2
$\mathbf{r}$	position vector to casting surface, m
R	universal gas constant, J/mole K
s	arc length along gap segment, m
t	time, s
u	mold filling speed, m/s
u_F	recession speed of foam above gap, m/s
v_B	bubble ascension speed, m/s
v_G	filter velocity of the gas diffusing through the coating, m/s
x	coordinate normal to flow front, m
x_C	fraction of the coating surface covered by non-wetting excess liquid polymer
x_V	mass fraction of polymer liquid vaporized in contact mode
z	vertical coordinate, m

Greek symbols

β	non-dimensional number in analysis of bubble flux
δ_A	mass flux fraction of air
δ_E	thickness of excess polymer liquid on the inside surface of coating, m
δ_V	mass flux fraction of polymer vapor
ε_M	emissivity of the metal surface
ε_P	energy per unit mass required to "melt" the foam, J/kg
ε_{PD}	energy per unit mass required to decompose the foam pattern, J/kg
ζ	distance below metal surface, m
ζ_0	distance below metal surface to furthest reach of excess polymer liquid, m
$\boldsymbol{\eta}$	bubble flux unit direction vector
θ	temperature of the liquid foam, K
θ_0	initial temperature of the pattern and sand, K
θ_G	average temperature of the gas in the gap, K
θ_M	temperature on the metal surface, K
θ_P	nominal melting temperature of the foam pattern, K
κ_C	gas permeability of the coating, m^2
λ_G	Peclet number in the gap
μ_G	viscosity of the gas escaping through the coating, Pa s
μ_L	viscosity of the polymer liquid diffusing through the coating, Pa s
ν	kinematic viscosity of the liquid metal, m^2/s
ξ^α	curvilinear coordinates on the casting surface
ρ_A^0	density of the air in the pattern at its initial pressure and temperature, kg/m^3
ρ_B	density of the gas in the bubbles, kg/m^3
ρ_F	partial density of the polymer in the foam, kg/m^3
ρ_P	total density of the foam pattern, kg/m^3
ρ_S	density of the polymer in the foam, kg/m^3
σ	Stephan–Boltzman constant, W/m^2 K^4
φ	volume fraction of air in the foam
φ_C	open porosity of the coating
φ_S	porosity of the sand

the polymer liquid, leaving the remainder to collect on its inside surface. The advancing liquid metal eventually overtakes this excess polymer liquid and begins to vaporize it, forming small gas bubbles that rise through the mold cavity. When these bubbles reach another flow front higher up in the cavity, they accumulate to form a finite gap between the liquid metal and the receding foam. As the gap widens, heat conduction from the metal to the foam is reduced, the filling speed slows down, and the foam begins to recede by melting rather than by ablation. When this happens, we say that the foam decomposes in *gap mode*.

Since a finite gap of this kind between the liquid metal and the receding surface of the foam is first created and then later sustained by gas bubbles that percolate through the liquid metal from remote locations in the cavity, gap mode is intrinsically *non-local*. A mathematical model for the mechanics of gap mode must not only account for heat transfer and mass diffusion along the immediate flow front, but also for polymer vaporization and the buoyant flux of vapor bubbles from other parts of the mold cavity.

Fig. 1 shows a neutron radiography image [4] taken during mold filling of a 12-mm thick rectangular plate with planar dimensions of 150×200 mm. The hydrogenous polystyrene foam shows up as a faint gray color on the neutron radiography image. Ordinarily, molten aluminum does not attenuate the neutron beam, but in this case it was doped with a small amount of gadolinium to make it visible as well. Instead of spreading outward in all directions from the inlet as it does in thinner plates, the metal flows down and across the plate, with the upper flow front remaining almost stationary. While this happens, a growing region of the N-ray image above the upper flow front changes from a uniform light intensity to a patchy whiter color interspersed with dark. The more-or-less level upper surface of the liquid metal does not begin to ascend until the right-facing flow front gets about halfway across the plate, and even then it advances at a much slower velocity.

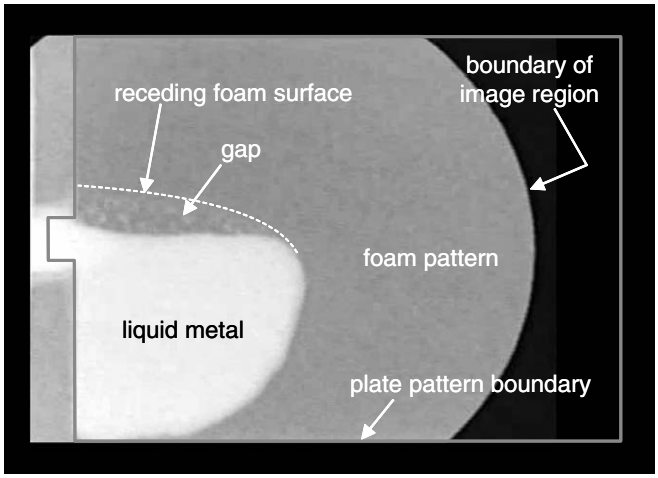

Fig. 1. Neutron radiography image of a 12-mm thick plate filling from the side, showing evidence of a distinct gap forming over the upper surface of the liquid metal.

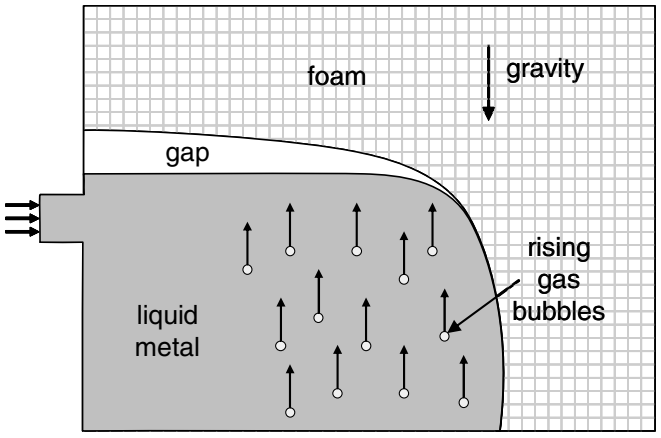

Fig. 2. Schematic illustration of the physical mechanisms at work during side filling of a thick, rectangular plate pattern.

Fig. 2 shows a schematic illustration of the physical mechanisms responsible for the filling sequence observed in Fig. 1. When a simple plate pattern thicker than about 8 mm fills from the side, the coatings normally used in aluminum casting do not have enough porous capacity to absorb all the residual liquid produced by the decomposing foam, leaving the rest to vaporize in small bubbles from the inside surface of the coating after the liquid metal passes by. These bubbles rise within the metal until they reach the upper flow front, where they collect to form a gap between the liquid metal and the unmelted foam. Just above the gap, the foam pattern continues to recede by melting away from the near-stationary metal surface. The residual polymer liquid produced by the melting foam collects in isolated globules on the inside surface of the coating, forming the area of patchy light intensity visible on the N-ray image in Fig. 1. The presence of a finite, connected gas layer along the upper flow front levels the surface of the liquid metal and slows down the upward rate of foam decomposition. This creates an asymmetric filling pattern in which the metal fills down and across the bottom of the pattern before moving upward. In thinner patterns, where the coating is able to absorb all the excess liquid, no gas bubbles form, and the metal fills symmetrically away from the inlet.

This paper presents a model for heat conduction, convection, and radiation between the liquid metal and the decomposing foam pattern in gap mode. The changing width of the gap is determined by a balance among the polymer vapor bubbling through the surface of the liquid metal from below, the air released from the foam as it melts from above, and the gas that escapes through the exposed coating in between. The bubble flux through the liquid metal is also modeled, including the loss of some polymer vapor by diffusion through the coating as it ascends. An analytical solution is obtained for the specific case of a uniform plate filling from the bottom. The results not only compare well with experimental data for aluminum alloys, but they also help to explain how part thickness, metal

temperature, and pressure affect filling speeds in patterns filling from the bottom.

2. The gap

2.1. Structure and composition

Consider the steady progress of foam decomposition in gap mode shown by the section through the pattern thickness illustrated in Fig. 3. The pattern recedes as the heat flux from the liquid metal melts the cellular structure of the foam above it. Experiments suggest that the foam surface actually arches over the liquid metal in this mode [5], so that the polymer liquid formed as the pattern melts does not have to flow towards the coating in a continuous stream. Instead, the melting polymer gathers, due to its own surface tension, into small beads on the surface of the foam, and these beads are transported to the coating en masse on the receding—and increasingly oblique—surface of the foam. The foam insulates the coating from the heat of the liquid metal until just before the last of it melts away, keeping the coating relatively cool and preventing the beads of liquid polymer from wetting the inside surface of the coating when they finally get there [6,7]. The polymer liquid collects in small, isolated globules on the inside surface of the coating, interspersed by regions of exposed coating through which the gas in the gap is able to escape into the surrounding sand. Eventually, the liquid metal overtakes the globules of liquid and they too begin to vaporize, creating gas bubbles of their own. Some of this gas diffuses through the coating between the globules as it ascends [7]. The rest reaches the surface of the liquid metal, adding to the gas already in the gap. In this way, even though the vapor bubbles that originally created the gap may cease, gap mode continues to sustain itself by producing excess liquid of its own that ultimately vaporizes and finds its way back into the gap. We assume that none of the polymer liquid vaporizes inside the gap itself.

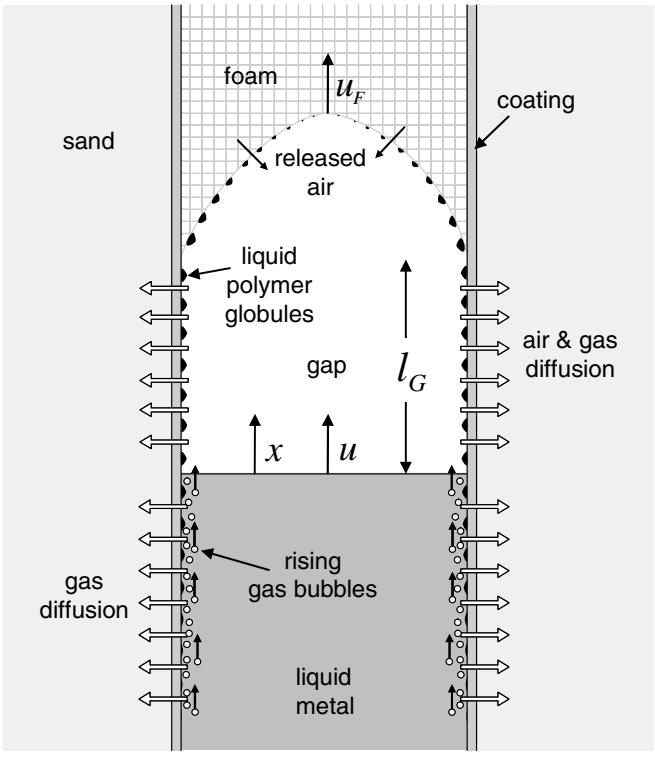

Fig. 3. Schematic illustration of foam decomposition in gap mode.

Although the foam pattern may contain residual blowing agents left over from the molding process [8], we assume that by the time the casting is poured nearly all these gases have diffused out of the foam, so that the pattern is composed entirely of solid polymer and air. Let φ denote the volume fraction of air in the foam, ρ_S the mass density of the polymer material, and ρ_A^0 the density of air at the initial pattern temperature θ_0 and atmospheric pressure p_0. Then the total density ρ_P of the foam pattern is given by

$$\rho_P = \varphi\rho_A^0 + (1-\varphi)\rho_S = \varphi\rho_A^0 + \rho_F, \tag{2.1}$$

where $\rho_F = (1-\varphi)\rho_S$ is the partial density of the polymer in the foam.

We assume that the gas pressure in any contiguous segment of the gap is uniform and equal to the pressure p_M at the surface of the liquid metal. For the relatively slow filling speeds in lost foam casting (about 1 cm/s) the metal pressure is quasi-static, and so the metal surface below the gap should be a level plane. The metal moves upwards at velocity u, and the foam recedes above it with velocity u_F. Let the origin of coordinates move with the surface of the liquid metal and let the x-axis be perpendicular to this surface, pointing towards the foam (Fig. 3). We neglect all temperature gradients parallel to the surface of the metal compared with the much steeper gradients across the width of the gap. Let θ_M denote the temperature on the surface of the liquid metal and θ_0 the uniform temperature of the pattern before the casting is poured. Even though most foam materials are glassy polymers without a well-defined melting temperature, they usually soften and then liquefy over a fairly narrow temperature range [9]. Hence we assume that on the receding foam surface, the foam reaches a nominal melting temperature designated by θ_P. Unless otherwise indicated, all temperatures and pressures in this paper are taken to be absolute quantities.

Let ε_P denote the energy per unit mass required to heat the foam from its initial temperature θ_0 to its "melting" temperature θ_P. If we let c_S denote the specific heat per unit mass of the solid polymer and H_M its latent heat of fusion, then it follows that

$$\rho_P\varepsilon_P = \left(\varphi\rho_A^0 c_A + \rho_F c_S\right)(\theta_P - \theta_0) + \rho_F H_M. \tag{2.2}$$

Since most foam materials are amorphous polymers, their latent heat of fusion is usually negligible. In particular, Tseng and Askeland [10] and Mehta et al. [9] detected no significant melting energy in laboratory experiments with polystyrene foam.

For simplicity in the analysis, we ignore the arched shape of the foam surface above the liquid metal and assume that the gap width l_G is uniform through the pattern thickness. The changing gap width is determined by the kinematic expression

$$\frac{dl_G}{dt} = u_F - u. \tag{2.3}$$

2.2. Heat conduction

We assume that as the foam melts ahead of the liquid metal, all of the air it originally contains enters the gap, where it diffuses into the sand through the exposed areas of the coating between the globules of residual liquid. In other words, no air escapes ahead of the metal through any open porosity that may be present in the unmelted foam. We assume that no polymer vapor in the gap is able to do so, either. The validity of this assumption depends on the quality of the molded foam [11,12].

Let m_V denote the mass flux of polymer vapor per unit area entering the gap through the surface of the liquid metal from below and m_A the corresponding mass flux of air released by the foam as it melts from above. Now m_V is determined by a separate analysis of the vaporizing liquid behind the metal front (considered in the next section), but m_A is given by

$$m_A = \varphi \rho_A^0 u_F. \tag{2.4}$$

If we assume that both these mass fluxes decrease linearly with distance across the gap, that heat conduction through the gap is quasi-steady, and that any tangential temperature gradients are negligible, then the energy balance equation for the gas temperature θ in the gap is given by

$$k_G \frac{\partial^2 \theta}{\partial x^2} + [c_A m_A (x/l_G) - c_V m_V (1 - x/l_G)] \frac{\partial \theta}{\partial x} = 0, \tag{2.5}$$

where k_G is the thermal conductivity of the gas mixture in the gap, and c_A and c_V are the specific heats of the air and polymer vapor, respectively. For simplicity, we assume that all these properties are approximately constant across the width of the gap. The boundary conditions are

$$\theta(0) = \theta_M, \quad \theta(l_G) = \theta_P. \tag{2.6}$$

The solution of (2.5) that satisfies the two boundary conditions in (2.6) is

$$\theta = \theta_M - \frac{\operatorname{erf}[\lambda_G(x/l_G - \delta_V)] + \operatorname{erf}(\lambda_G \delta_V)}{\operatorname{erf}(\lambda_G \delta_V) + \operatorname{erf}(\lambda_G \delta_A)} (\theta_M - \theta_P), \quad 0 \leqslant x \leqslant l_G, \tag{2.7}$$

where

$$\lambda_G^2 = \frac{l_G}{2k_G}(c_A m_A + c_V m_V), \tag{2.8}$$

$$\delta_A = \frac{c_A m_A}{c_A m_A + c_V m_V}, \quad \delta_V = 1 - \delta_A = \frac{c_V m_V}{c_A m_A + c_V m_V}. \tag{2.9}$$

The conduction heat flux corresponding to (2.7) is

$$q(x) = -k_G \frac{\partial \theta}{\partial x} = \frac{k_G}{l_G} \frac{2}{\sqrt{\pi}} \frac{\lambda_G e^{-[\lambda_G (x/l_G - \delta_V)]^2}}{\operatorname{erf}(\lambda_G \delta_V) + \operatorname{erf}(\lambda_G \delta_A)} (\theta_M - \theta_P), \quad 0 \leqslant x \leqslant l_G. \tag{2.10}$$

At the surface of the receding foam, (2.10) becomes

$$q(l_G) = h_G(\theta_M - \theta_P), \tag{2.11}$$

where

$$h_G = \frac{k_G}{l_G} \frac{2}{\sqrt{\pi}} \frac{\lambda_G e^{-(\lambda_G \delta_A)^2}}{\operatorname{erf}(\lambda_G \delta_V) + \operatorname{erf}(\lambda_G \delta_A)} \tag{2.12}$$

represents an effective heat transfer coefficient between the liquid metal and surface of the unmelted foam.

In addition to the conduction heat flux (2.11), the foam is also subjected to radiation from the liquid metal. Let q_R represent the average radiation heat flux incident on the surface of the unmelted foam. Then

$$q_R = F \sigma \varepsilon_M \theta_M^4, \tag{2.13}$$

where σ is the Stephan–Boltzman constant, ε_M is the emissivity of the metal surface and F is the geometric view factor between the metal surface and the foam. Here we assume that all incident radiation is absorbed by the foam and neglect any radiation emitted by the foam itself. As long as the gap width varies slowly along the flow front, the view factor may be computed based on two-dimensional considerations alone. If d represents the pattern thickness, then it is a simple matter to show that [13]

$$F = \sqrt{1 + (l_G/d)^2} - l_G/d. \tag{2.14}$$

The view factor, and hence also the radiation heat flux, decreases as the gap widens.

Since the combined heat flux from conduction and radiation must sustain the recession rate of the foam pattern, we have

$$h_G(\theta_M - \theta_P) + q_R = \rho_P \varepsilon_P u_F. \tag{2.15}$$

For a given value of the polymer vapor flux m_V and gap width l_G, this equation, together with (2.4), (2.8), (2.9), and (2.12)–(2.14), determines the rate of foam decomposition u_F at any point along a segment of the flow front in gap mode.

The heat flux q_M from the metal surface, which follows from (2.10), is

$$q_M = q(0) + \sigma \varepsilon_M \theta_M^4 = \frac{k_G}{l_G} \frac{2}{\sqrt{\pi}} \frac{\lambda_G e^{-(\lambda_G \delta_V)^2}}{\operatorname{erf}(\lambda_G \delta_V) + \operatorname{erf}(\lambda_G \delta_A)} (\theta_M - \theta_P) + \sigma \varepsilon_M \theta_M^4. \tag{2.16}$$

This equation provides the thermal boundary condition for the heat conduction problem in the liquid metal. For gap mode the *pattern decomposition energy* ε_{PD} is given by

$$\varepsilon_{PD} = \frac{q_M}{\rho_P u_F}. \tag{2.17}$$

The decomposition energy in gap mode is significantly smaller than in contact mode [3] because in gap mode all of the polymer vaporization occurs behind the metal front.

The only quantity that is still undetermined is the metal velocity u. Since the surface of the liquid metal must remain horizontal along any contiguous segment of the flow front in gap mode, this velocity has a single value over the entire segment. To determine this value, we need to consider a mass balance for the gas mixture in the gap segment.

2.3. Balance of gas volume

Ordinarily, the balance of mass in the gap involves separate equations for the air and polymer vapor. As long as the pressure, temperature, and composition of the gas in the gap are all reasonably steady, though, the gas densities do not vary significantly with time and the separate mass balance equations for the air and polymer vapor are equivalent to an overall balance of volume for the gas mixture as a whole. We assume that the volume rate of incoming air released by the receding foam plus the volume rate of incoming vapor (both adjusted for the average temperature along the gap segment) less the volume rate of combined gas escaping through the coating equals the rate of change of the total gap volume.

Consider a contiguous segment of the flow front where the foam is decomposing in gap mode. From (2.7) the average gas temperature θ_G in the gap is

$$\begin{aligned}\theta_G &= \frac{1}{l_G}\int_0^{l_G}\theta(x)\,dx \\ &= \theta_P + \left[\delta_V - \frac{1}{\sqrt{\pi}\lambda_G}\frac{e^{-(\lambda_G\delta_A)^2} - e^{-(\lambda_G\delta_V)^2}}{\operatorname{erf}(\lambda_G\delta_V) + \operatorname{erf}(\lambda_G\delta_A)}\right](\theta_M - \theta_P).\end{aligned} \tag{2.18}$$

Assuming the air and polymer vapor both behave as ideal gases, we have for their respective densities

$$\rho_A = \rho_A^0\frac{p_M\theta_0}{p_0\theta_G}, \quad \rho_V = \frac{p_M M_V}{R\theta_G}, \tag{2.19}$$

where M_V is the average molecular weight of the polymer vapor bubbling up through the liquid metal and R is the universal gas constant.

As in contact mode [3], we assume that gas diffuses through the coating according to Darcy's law [14]. And, just as in contact mode, we neglect the diffusive resistance of the sand compared with that of the coating. Hence the filter velocity v_G of the gas through the open sections of the coating in the gap is given by [3]

$$v_G = \frac{\kappa_C}{\mu_G d_C}\frac{p_M^2 - p_S^2}{2p_M}, \tag{2.20}$$

where κ_C is the permeability of the coating, d_C is its thickness, μ_G is the viscosity of the gas mixture, and p_S is the pressure in the sand.

Now if we let x_C denote the fraction of the coating surface covered by the globules of liquid polymer, the overall balance of volume for the gas mixture in the gap segment is expressed by

$$\int_\Gamma [m_V d/\rho_V + m_A d/\rho_A - (u_F - u)d - 2(1 - x_C)v_G l_G]\,ds = 0, \tag{2.21}$$

where s denotes arc length along the gap segment Γ. Together with the heat conduction solution in the previous section, this equation determines the vertical velocity u of the metal surface. Note that for large values of m_V, the metal velocity actually could be negative. This would be temporary, though, since a negative metal velocity widens the gap (u_F must always be positive), which exposes more coating surface area to gas diffusion.

3. Polymer vaporization and bubble flux

3.1. Residual liquid

The ultimate fate of any residual polymer liquid left behind on the inside of the coating as the metal advances through the pattern depends on how the pattern decomposes at a particular location. If the pattern decomposes in contact mode, then the gas is able to diffuse through the coating in the undercut ahead of the metal front [3], heating the coating sufficiently for the residual liquid to wet its inside surface [6]. Several investigators have also observed residual liquid penetrating the coating either by capillary forces or by the direct pressure from the liquid metal [6,7]. Once the coating absorbs the polymer liquid, it should be much harder for the liquid to vaporize and reenter the metal stream. The fact that gap mode is observed almost exclusively in patterns thicker than about 8 mm suggests that the coating successfully absorbs all the residual liquid in thinner parts, keeping it from vaporizing inside the mold cavity and preventing polymer vapor from bubbling through the liquid metal.

To explore this concept further, we let φ_C denote the open porosity of the coating and x_V the mass fraction of polymer vapor created when the foam decomposes in contact mode. Then the coating is able to absorb *all* the residual liquid created in contact mode provided

$$d < \frac{2\varphi_C d_C}{(1 - x_V)(1 - \varphi)}. \tag{3.1}$$

For the typical value $x_V = 1/3$ [3] and the properties listed in Tables 1 and 2, the critical thickness turns out to be about 8 mm, consistent with the observation noted above. With this as primary motivation, then, we assume that cap-

Table 1
Material properties of polystyrene foam

Property	Symbol	Value	Unit
Nominal foam density	ρ_F	25	kg/m^3
Polymer density	ρ_S	800	kg/m^3
Melting temperature	θ_P	150	°C
Melting energy	H_M	0	J/g
Specific heat of solid	c_S	1.5	J/g K
Specific heat of vapor	c_V	2.2	J/g K
Vaporization rate	γ	0.02	kg/m^2 s
Molecular weight of vapor	M_V	104	g/mole
Coating coverage fraction	x_C	0.5	
Thermal conductivity of gas	k_G	0.04	W/m K
Viscosity of gas	μ_G	2×10^{-5}	Pa s

Table 2
Material properties of coating

Property	Symbol	Value	Unit
Permeability	κ_C	0.02	μm^2
Porosity	φ_C	0.4	
Thickness	d_C	0.2	mm

illary pressures are sufficient to draw residual liquid into the open pores of the coating until either the coating saturates completely or all the residual liquid is exhausted. We further assume that all the liquid wicks into the coating before any of it has a chance to vaporize and bubble into the liquid metal. Let δ_E denote the thickness of the *excess liquid* remaining on the inside of the coating after the coating saturates. Then according to the assumptions above

$$\delta_E = \frac{1}{2}(1-x_V)(1-\varphi)d - \varphi_C d_C \quad \text{(contact mode)}. \tag{3.2}$$

The situation in gap mode is entirely different. Here there is no gas produced as the foam decomposes and the coating is too cool for the polymer liquid to even wet its inside surface, much less wick inside. Instead the polymer liquid collects in globules on the inside surface of the coating [7], covering some fraction, say x_C, of the coating surface. In this case all the residual liquid is excess liquid and the average thickness of the liquid in the globules is

$$\delta_E = \frac{1}{2x_C}(1-\varphi)d \quad \text{(gap mode)}. \tag{3.3}$$

Eqs. (3.2) and (3.3) determine the initial thickness of the excess liquid before any further liquid diffuses through the coating or any vaporization occurs. Let γ denote the mass rate of vaporization per unit area of the excess liquid into the liquid metal. Where the pattern decomposes in contact mode, we assume that the excess liquid continues to diffuse into the coating according to Darcy's law. Then as long as excess liquid remains on the coating ($\delta_E > 0$), its thickness changes according to

$$\rho_S\frac{\partial\delta_E}{\partial t} + \gamma + \frac{\rho_S\kappa_C}{\mu_L d_C}(p_M - p_S) = 0 \quad \text{(contact mode)}, \tag{3.4}$$

where μ_L represents the viscosity of the polymer liquid. Where the pattern decomposes in gap mode, the pools of liquid polymer prevent the coating from getting hot enough for the liquid to penetrate [7], and the excess liquid satisfies the simpler equation

$$\rho_S\frac{\partial\delta_E}{\partial t} + \gamma = 0 \quad \text{(gap mode)}. \tag{3.5}$$

The viscosity μ_L of the polymer liquid is quite sensitive to its molecular weight and temperature, while the rate of vaporization γ is likely to depend on both the temperature and pressure of the liquid metal.

3.2. Bubble flux through the liquid metal

When the liquid metal overtakes the excess polymer liquid along the inside of the coating, the polymer begins to vaporize, forming small bubbles that nucleate on the surface of the polymer liquid and then rise due to their buoyancy in the much denser liquid metal. There is ample evidence for the formation and ascent of gas bubbles in lost foam casting, both in experiments behind glass windows [15–17] and in the agitated surface of the liquid metal visible in real-time X-ray images as the gas bubbles break through the free surface of the liquid metal and enter an open gap above it. Sands and Shivkumar [17] observed bubble diameters between 0.5 and 2 mm in their glass-window experiments. Small gas bubbles of radius a_B rise in a dense viscous liquid at the rate [18]

$$v_B = \frac{a_B^2 g}{3\nu}, \tag{3.6}$$

where g is the acceleration of gravity and ν is the kinematic viscosity of the liquid. This means that for millimeter-size bubbles in liquid aluminum, which has a kinematic viscosity of about 10^{-6} m^2/s, bubbles rise at the rate of about 1 m/s. Since this speed is about two orders of magnitude faster than the usual rate of foam decomposition, it is reasonable to assume a quasi-steady mass balance for the bubbles rising in the liquid metal.

To formulate the equations governing the motion of the gas bubbles, we must first characterize the geometry of the mold cavity. Consistent with the idealizations implicit in the foam decomposition model considered here and by Barone and Caulk [3], we idealize the mold cavity as a shell-like region represented by a surface in space, called the *casting surface*, together with an associated thickness d that may vary from point to point (Fig. 4). Let ξ^α ($\alpha = 1, 2$) be curvilinear coordinates on the idealized casting surface and let $\mathbf{r}(\xi^\alpha)$ denote the position vector to any point ξ^α on that surface. We assume that the bubbles rise along a direction parallel to the projection of the vertical unit vector $\mathbf{k}$ on the local tangent plane of the casting surface $\mathbf{r}$. Let z denote the vertical distance from the origin, so that $\mathbf{r}\cdot\mathbf{k} = z$. Then

$$\mathbf{r}_{,\alpha}\cdot\mathbf{k} = \mathbf{a}_\alpha\cdot\mathbf{k} = z_{,\alpha}, \tag{3.7}$$

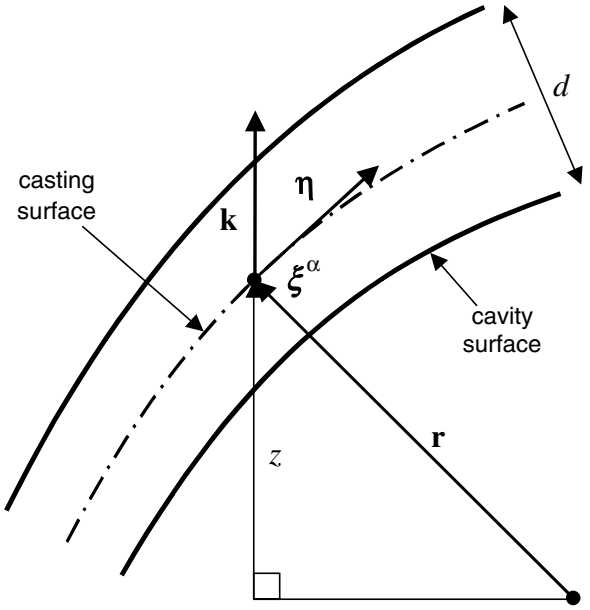

Fig. 4. Geometry of the mold cavity for the bubble flux formulation.

where $\mathbf{a}_\alpha$ are the covariant base vectors on the casting surface corresponding to the coordinates ξ^α. Since the base vectors are tangent to the surface, it follows that the bubbles rise parallel to the unit vector

$$\boldsymbol{\eta}(\xi^\alpha) = \frac{z_{,\alpha}\mathbf{a}^\alpha}{\left(a^{\beta\gamma}z_{,\beta}z_{,\gamma}\right)^{1/2}}, \tag{3.8}$$

where $\mathbf{a}^\alpha$ are the contravariant base vectors and $a^{\alpha\beta}$ are the contravariant components of the surface metric tensor. Note that the unit vector $\boldsymbol{\eta}$ is not defined at points where the surface is locally horizontal.

Now let $\mathbf{m}(\xi^\alpha)$ denote the local mass flux vector of bubbles per unit length along the casting surface, or more simply the *bubble flux vector*. According to the above assumptions, $\mathbf{m}$ is directed parallel to $\boldsymbol{\eta}$. Hence we can write

$$\mathbf{m} = m(\xi^\alpha)\boldsymbol{\eta}. \tag{3.9}$$

The scalar function $m(\xi^\alpha)$ is called the *bubble flux*. At points where the tangent plane is horizontal, it is reasonable to expect the bubble flux vector to vanish, and so here we set $m = 0$ and avoid the ambiguity of an undefined $\boldsymbol{\eta}$. Before formulating an equation governing the bubble flux m, we must first consider the possible diffusion of gas from the bubbles through exposed areas of the coating between the globules of excess liquid as they ascend.

3.3. Bubble diffusion through the coating

After the bubbles nucleate, they should stay fairly close to the coating as they rise since bubbles that touch the coating share less surface area with the liquid metal and hence require less surface energy per unit volume of gas. When the bubbles encounter exposed areas of coating as they rise, though, some of their gas can diffuse through the coating and into the surrounding sand, subtracting from the local bubble flux. Let $m_C(\xi^\alpha)$ denote the mass flux of gas per unit area diffusing through the coating from the bubble stream at the point ξ^α. Intuitively we would expect m_C to increase with the local bubble density and the metal pressure.

To motivate an explicit constitutive equation for m_C, consider the idealized case where the bubbles are all hemispheres of radius a_B, with their flat side adjacent to the coating. Then the area of contact between the bubbles and the coating per unit volume of the gas is $3/2a_B$. If we further assume that both sides of the cavity share the bubble flux equally, then the mass density of bubbles per unit area of the coating is $m/2v_B$. Hence the fraction of the coating surface actually exposed to the gas in the bubbles is

$$\frac{3m}{4\rho_B v_B a_B}, \tag{3.10}$$

where ρ_B is the density of the gas in the bubbles. Then with (3.6), the mass flux of gas diffusing through the coating should be given by

$$m_C = \rho_B v_G \frac{3m}{4\rho_B v_B a_B} = \left[\frac{9\nu}{4a_B^3 g}\right] v_G m, \tag{3.11}$$

where v_G is specified by (2.20). Note that the bracketed term in (3.11) depends only on the properties of the liquid metal. With this as motivation, we assume that in general m_C is specified by the constitutive equation

$$m_C = \kappa_B v_G m, \tag{3.12}$$

where the coefficient κ_B is a constant. We call m_C the *bubble diffusion flux* and κ_B the *bubble diffusion coefficient*. Although (3.11) was derived only to motivate (3.12), we note that for millimeter-size bubbles and a kinematic viscosity for the liquid metal of 10^{-6}, the bracketed term in (3.11) is $O(10^3)$ s/m^2. This should give us some expectation for at least the order of magnitude of the bubble diffusion coefficient.

Considering the vaporization of additional gas from the excess liquid and the bubble diffusion flux defined by (3.12), the overall balance of mass for the gas bubbles in the liquid metal is expressed by

$$2x_C\gamma - 2(1-x_C)\kappa_B v_G m = \nabla\cdot(m\boldsymbol{\eta}), \tag{3.13}$$

where $\nabla = \mathbf{a}^\alpha\partial/\partial\xi^\alpha$ is the divergence operator on the casting surface. When the bubbles break through the flow front, the mass flux of gas entering the corresponding gap segment is given by

$$m_V = m/d. \tag{3.14}$$

4. One-dimensional bottom fill solution

4.1. Geometry and coordinates

To see how the various physical mechanisms described in the previous two sections combine to affect filling speed, it is instructive to consider a simple one-dimensional example where the foam decomposes exclusively in gap mode.

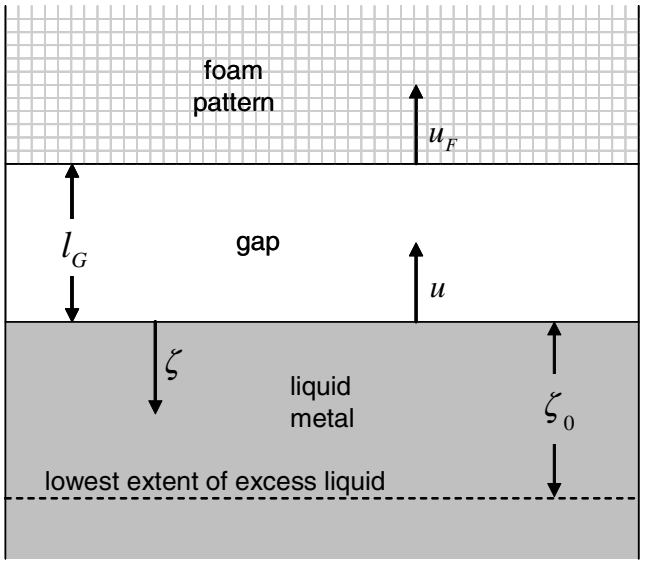

Fig. 5. One-dimensional bottom filling in gap mode.

Fig. 5 illustrates a uniform pattern of thickness d oriented vertically in the mold and filling uniformly from the bottom. Even if the foam starts decomposing in contact mode, the excess liquid (when it exists) vaporizes below the flow front and the rising bubbles eventually reach the metal surface and create a gap. We let ζ measure depth below the level surface of the liquid metal and assume that all the excess liquid is completely vaporized below $\zeta = \zeta_0$.

For simplicity, we assume that the vaporization rate γ and the coating coverage fraction x_C are both constant (Table 1). The vaporization rate (0.02 kg/m^2 s) was determined indirectly by observing how long gas bubbles continue to agitate the metal surface below the gap in X-ray images of mold filling in situations like that in Fig. 1. This value is also consistent with measurements by Shivkumar and Gallois [19] under slightly different conditions. The coating coverage fraction was estimated based on photographs in [5]. The bubble diffusion coefficient is more difficult to determine from direct observations, so for now we simply set it equal to 500 s/m^2 (Table 3) based on the analysis leading to (3.12).

Since time is interchangeable with flow-front position as a measure of mold filling progress in this problem, the changing gap width in (2.3) may be expressed in the alternative form

$$-\frac{\partial l_G}{\partial \zeta} u = u_F - u. \tag{4.1}$$

Table 3
Material properties of molten aluminum

Property	Symbol	Value	Unit
Mass density	ρ_M	2500	kg/m^3
Surface emissivity	ε_M	0.6	
Bubble diffusion coefficient	κ_B	500	s/m^2

4.2. Bubble flux solution

In this case the bubble flux m depends only on the depth coordinate, and so (3.13) reduces to

$$-\frac{\partial m}{\partial \zeta} + 2(1 - x_C)\kappa_B v_G m = 2x_C\gamma. \tag{4.2}$$

For simplicity, we approximate (2.20) by the linear form

$$v_G = \frac{\kappa_C}{\mu_G d_C}(p_M - p_S), \tag{4.3}$$

which is valid when the head pressure

$$p_M - p_S = \rho_M g(H + \zeta) \tag{4.4}$$

is small compared with p_S. In (4.4), ρ_M is the density of the liquid metal, g is the acceleration of gravity, and H is the uniform metal head along the flow front. Combining (4.2)–(4.4), we obtain

$$-\frac{\partial m}{\partial \hat{\zeta}} + 2\beta^2(1 + \hat{\zeta})m = 2x_C H\gamma, \tag{4.5}$$

where

$$\beta^2 = \rho_M g H^2 \frac{\kappa_B \kappa_C}{\mu_G d_C}(1 - x_C) \tag{4.6}$$

and $\hat{\zeta}$ is a non-dimensional depth coordinate defined by

$$\hat{\zeta} = \zeta/H. \tag{4.7}$$

Since there is no excess liquid below $\zeta = \zeta_0$, the boundary condition for (4.5) is

$$m(\hat{\zeta}_0) = 0. \tag{4.8}$$

The solution of (4.5) that satisfies (4.8) is

$$m(\hat{\zeta}) = \frac{x_C H\gamma\sqrt{\pi}}{\beta} e^{\beta^2(\hat{\zeta}+1)^2}\{\mathrm{erf}[\beta(\hat{\zeta}_0 + 1)] - \mathrm{erf}[\beta(\hat{\zeta} + 1)]\}. \tag{4.9}$$

In Fig. 6 we plot the non-dimensional bubble flux $m/x_C H\gamma$ from (4.9) as a function of the non-dimensional depth $\hat{\zeta}$ for $\beta = 3$ and various depths of residual liquid.

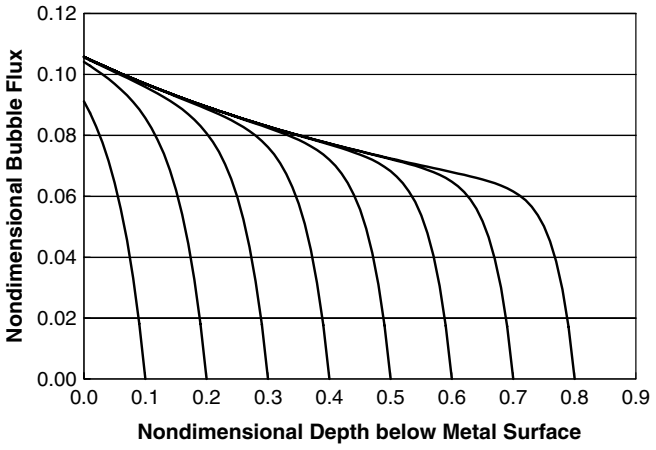

Fig. 6. Non-dimensional bubble flux $m/x_C H\gamma$ from (4.9) for various depths of residual liquid ζ_0/H and $\beta = 3$.

The value for β is based on a metal head of about 0.5 m and the material properties listed in Tables 1–3. A very interesting trend emerges from these results. A short distance above the lowest reach of the excess liquid, the curves for the different depths coalesce and the bubble flux becomes independent of ζ_0. This is a direct result of the constitutive equation (3.12) for the bubble flux diffusion. If there were no bubble diffusion, the second term on the left-hand side of (4.5) would vanish and the solution for m would increase linearly with distance above the bottom edge of the residual liquid. We see just such a trend in Fig. 6 very near $\zeta = \zeta_0$. But with increasing distance above ζ_0, a growing bubble flux allows more gas to diffuse through the coating, reducing its rate of growth. Far enough up, a balance is reached between additional vaporization and losses to diffusion that nullifies any further sensitivity of the bubble flux to ζ_0. This result has important consequences later when we consider bubble flux into the gap and its ultimate effect on filling speed.

4.3. Balance of gas in the gap

From (4.9) the bubble flux into the gap is given by

$$m(0) = m_V d = \frac{x_C H\gamma\sqrt{\pi}}{\beta} e^{\beta^2}\{\mathrm{erf}[\beta(\hat{\zeta}_0 + 1)] - \mathrm{erf}(\beta)\}. \tag{4.10}$$

Fig. 7 plots the non-dimensional bubble flux $m(0)/x_C H\gamma$ from (4.10) as a function of the non-dimensional excess liquid depth $\hat{\zeta}_0$, again for $\beta = 3$. This curve reaches an asymptote shortly after the excess liquid extends about one-tenth of the metal head below the flow front. This means that even though thicker parts create more excess liquid, they still have the same amount of gas bubbling into the gap as thinner parts do. For some patterns, less than 20% of the vaporizing liquid ultimately reaches the gap. This result may explain why the metal surface appears less agitated in real-time X-ray images of bottom filling, compared with side filling for the same pattern thickness. In side filling the foam decomposes in contact mode, which enables the residual liquid to wet the coating, leaving no sections of the coating exposed for bubble diffusion to diminish the resultant bubble flux.

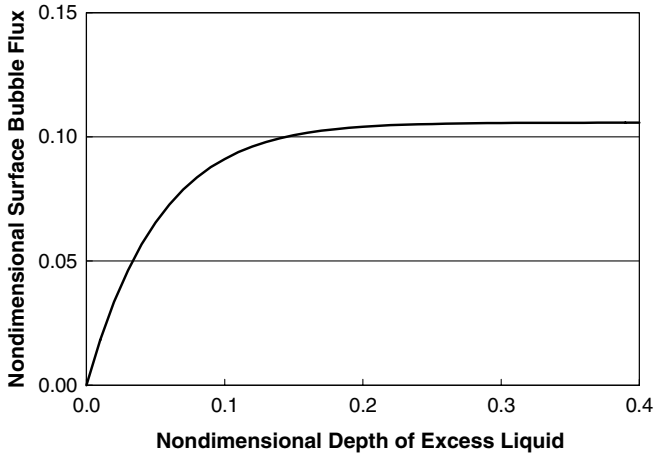

Fig. 7. Non-dimensional bubble flux into the gap $m(0)/x_C H\gamma$ from (4.10) as a function of the non-dimensional excess liquid depth ζ_0/H and $\beta = 3$.

By equating the time for the metal to travel a given distance through the pattern with the time it takes the excess liquid to completely vaporize, it is a straightforward matter to show that the depth ζ_0 of the residual liquid below the flow front is determined by

$$\int_0^{\zeta_0} \frac{\mathrm{d}\zeta}{u} = \frac{\rho_F d}{2x_C\gamma}. \tag{4.11}$$

In an actual bottom-fill process, the temperature and pressure of the metal decrease as it moves upward, causing the filling speed to slow down. When u is not constant, the integral equation (4.11) does not have an easy solution. For the present purpose, though, we assume that the filling speed does not change very much in the range $0 \leqslant \zeta \leqslant \zeta_0$, so that (4.11) may be approximated by the simpler expression

$$\zeta_0 = \frac{\rho_F d u}{2x_C\gamma}. \tag{4.12}$$

A solution based on this approximation (which always underestimates ζ_0) is actually much better than it might first appear. Clearly (4.12) is most accurate when ζ_0 is small. But we also know from the solution (4.10) that the bubble flux into the gap stops depending on ζ_0 when $\zeta_0/H > 0.1$. Hence, even though the error in (4.12) grows with increasing ζ_0, that error has a negligible effect on the rest of the solution.

With the help of (2.4), (2.19) and (4.1), the gas balance (2.21) in the gap reduces to

$$\frac{m(0)R\theta_G}{p_M M_V} + \frac{\varphi p_0 \theta_G u_F d}{p_M \theta_0} + \frac{\partial l_G}{\partial\zeta} ud - (1 - x_C)\frac{\kappa_C l_G}{\mu_G d_C p_M}\left(p_M^2 - p_S^2\right) = 0, \tag{4.13}$$

where $m(0)$ is given by (4.10) and θ_G by (2.18). In most cases the gap width is much smaller than the metal head, so that $\partial l_G/\partial\zeta \ll 1$. Hence (4.1) may be approximated by

$$u = u_F \tag{4.14}$$

and (4.13) further reduces to

$$\frac{m(0)R\theta_G}{p_M M_V} + \frac{\varphi p_0 \theta_G u d}{p_M \theta_0} - (1 - x_C)\frac{\kappa_C l_G}{\mu_G d_C p_M}\left(p_M^2 - p_S^2\right) = 0. \tag{4.15}$$

Likewise, (2.15) and (4.1) combine to give

$$h_G(\theta_M - \theta_P) + q_R = \rho_P \varepsilon_P u. \tag{4.16}$$

The two algebraic equations (4.15) and (4.16) determine the filling speed u together with the corresponding gap width l_G.

4.4. Results

Fig. 8 displays the solution for the filling speed as a function of the aluminum head at four values of the pattern thickness and a metal temperature of 700 °C, using the properties for polystyrene foam in Table 1, the coating in Table 2, and molten aluminum in Table 3. Even though gap mode is unlikely to develop for patterns as thin as 4 mm, we include this case anyway to be consistent with the thickness range considered for contact mode in [3].

The first thing that stands out in these results is that although filling speed has a strong, almost linear dependence on metal pressure, it is nearly unaffected by pattern thickness. This is especially true above 8 mm thick, where gap mode is more likely to occur anyway. This result apparently stems from two important differences between thick and thin parts that almost completely compensate for one another.

Because of the gas drawn off by bubble diffusion, we know that regardless of the pattern thickness, the amount of polymer vapor bubbling into the gap is about the same. The amount of air released by the receding foam, however, is not. Thicker parts release more air into the gap than thinner ones, requiring a wider gap to expel the air and sustain the same filling speed. A wider gap reduces heat conduction from the liquid metal, which ordinarily would slow the rate of foam melting and decrease filling speed. But the view factor (2.14) is higher in thicker parts, so that the reduced heat conduction is almost completely offset by higher radiation, leaving the filling speed unaffected.

According to Fig. 8, filling speeds vary from about 3 to 7 mm/s, depending on pressure. These values are about half as large as in contact mode [3]. Corresponding results for gap width are shown in Fig. 9. As expected, the gap widens as the pattern gets thicker and the pressure decreases.

These results are consistent with experimental observations with neutron radiography [4]. Fig. 10 shows a sample image taken during mold filling of the same 150 × 200-mm plate pattern in Fig. 1, but this time standing on end and filling from two inlets at the bottom. Fig. 11 compares tracings of the metal front positions at 2-second intervals in a 12-mm and a 24-mm plate. In all these cases, the metal temperature was about 700 °C and the metal head approximately 0.5 m. Not only are the filling speeds for both thicknesses about equal, but each is very close to 5 mm/s, consistent with the results in Fig. 8. The gap width is more difficult to make out, but it seems to be about 1 cm, consistent with the results in Fig. 9.

Fig. 12 shows the filling speed as a function of metal temperature for a constant metal head of 0.5 m. It turns out that filling speed responds strongly to metal temperature in gap mode, increasing by about 50% over the range 600–800 °C. This is mostly due to increased radiation. In contrast, filling speed has little or no dependence on metal

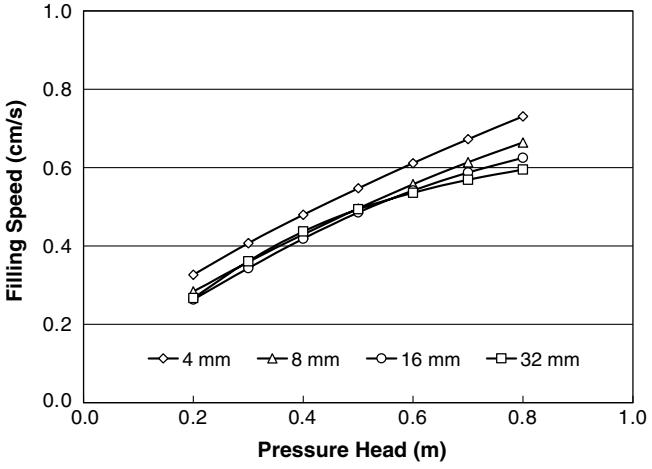

Fig. 8. Filling speed in gap mode as a function of metal pressure (in meters of aluminum) for various thicknesses of polystyrene foam and a metal temperature of 700 °C.

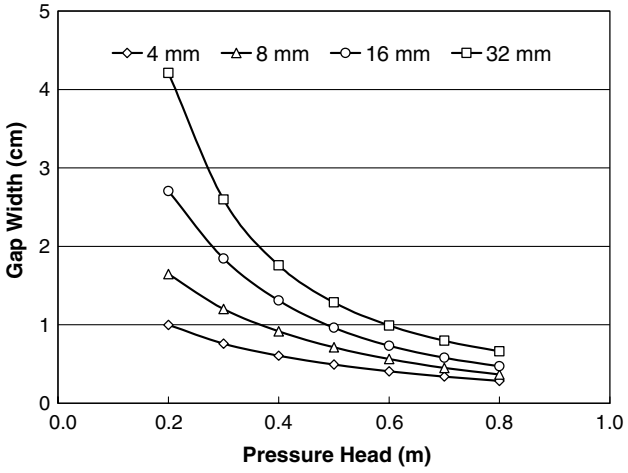

Fig. 9. Gap width as a function of metal pressure (in meters of aluminum) for various thicknesses of polystyrene foam and a metal temperature of 700 °C.

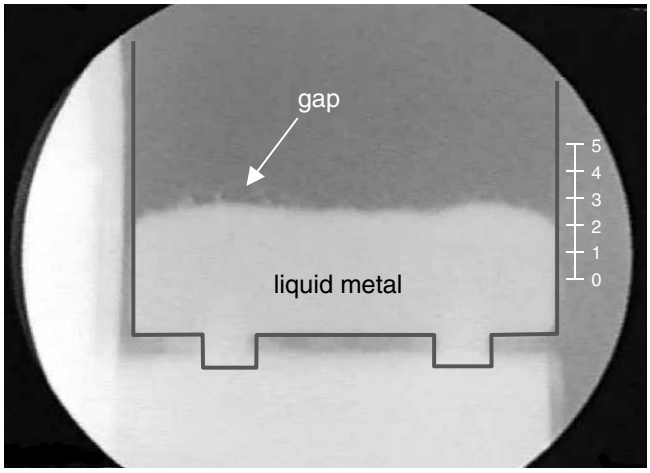

Fig. 10. Neutron radiography image of a 12-mm plate filling from the bottom. The scale on the right is in centimeters.

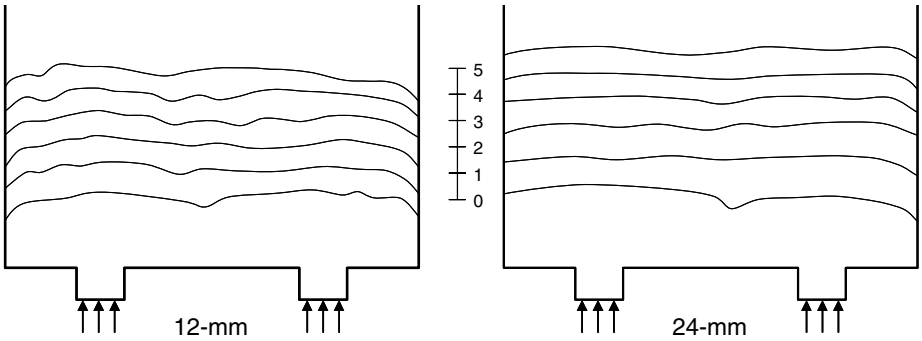

Fig. 11. Tracings of metal front position at 2-s intervals from neutron radiography images taken during bottom filling of 12- and 24-mm thick plate patterns. The scale is in centimeters.

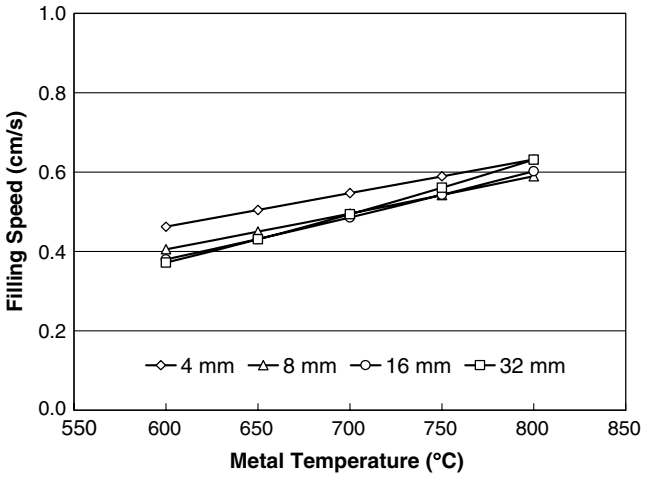

Fig. 12. Filling speed in gap mode as a function of metal temperature for various thicknesses of polystyrene foam and a metal pressure corresponding to 0.5 m of aluminum.

temperature in contact mode [3]. The dependence of gap width on metal temperature is shown in Fig. 13. The gap widens with increasing temperature, although not as much as it does with changes in pressure. Experimental results like those in Figs. 10 and 11 are not currently available for a variation in metal temperature.

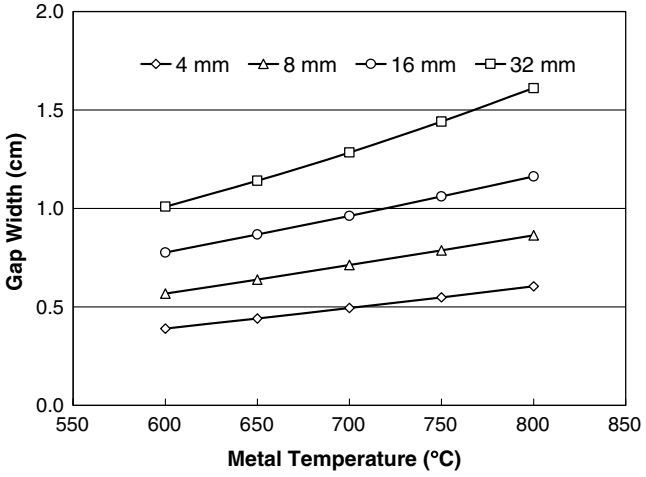

Fig. 13. Gap width as a function of metal temperature for various thicknesses of polystyrene foam and a metal pressure corresponding to 0.5 m of aluminum.

5. Discussion

This paper presents a model for the mechanics of foam decomposition in *gap mode* during mold filling in lost foam casting of aluminum. Gap mode develops when rising gas bubbles in the liquid metal collect along an upward-facing flow front, opening a finite gap between the liquid metal and the unmelted foam. The gas bubbles are created when the liquid metal vaporizes excess polymer liquid left behind on the inside surface of the coating as the pattern decomposes. After a distinct gas layer forms between the liquid metal and the foam in this way, the pattern can no longer decompose in *contact mode* and mold filling continues by an entirely different mechanism. Heat conduction decreases because of the widening gap, radiation suddenly becomes important, and the foam recedes by melting rather than by ablation.

An analytical solution is derived for the heat conduction equation in the gap, including the convection of polymer vapor entering the gap from below and the air released from above as the foam recedes. The heat flux across the gap, combined with radiation from the surface of the liquid metal, determines the rate of foam recession. Since the gas pressure in the gap is approximately uniform, the metal surface levels out and its further progress is determined by a balance of gas volume in the gap.

A model is proposed for the formation of excess liquid behind the metal front. Some of this liquid vaporizes when it contacts the liquid metal and (when the liquid is able to wet the coating) some diffuses through the coating and into the sand. As the bubbles rise in the mold cavity, some gas is drawn off by diffusion through areas of the coating not covered by liquid, thereby depleting the upward gas flux carried in the bubbles. A constitutive equation is proposed to govern this diffusion, involving a single coefficient that depends only on the properties of the liquid metal. A mass balance equation is formulated for the bubble flux through the liquid metal that applies to thin cavities of general shape.

The heat conduction and mass balance equations in the gap are solved together with the bubble flux equations in the liquid metal for the special case of one-dimensional bottom filling in gap mode. The filling speeds calculated from this solution are nearly linear in metal pressure, with almost no dependence on pattern thickness. Although the latter result is similar to contact mode, the reasons for it are entirely different here. As the pattern gets thicker, the receding foam releases more air per unit area of exposed coating, causing the gap to widen and the conduction heat flux to decrease. But the radiation flux increases at the same time because the view factor is larger in thicker parts. It turns out that these two effects very nearly compensate for one another, resulting in a negligible change in filling speed with part thickness.

The filling speeds themselves range from 3 to 7 mm/s in bottom fill, less than half those of contact mode, but nevertheless consistent with experimental observations with neutron radiography in bottom-filled polystyrene patterns coated with a mica-based refractory.

The calculated width of the gap is between 5 and 20 mm. It is wider for thicker parts and lower pressures, as expected. These widths are consistent with neutron radiation imagery on bottom-filled plate patterns. Unlike contact mode, the metal temperature in gap mode has as strong influence on filling speed, increasing it by 50% over the range 600–800 °C. This is primarily due to the strong role that radiation now plays in determining the rate of foam decomposition.

Acknowledgements

The author would like to thank Dr. David Goettsch of General Motors Powertrain for permission to publish some of his neutron radiography images, which were so helpful in formulating the physical assumptions in the foam decomposition model. Gratitude is also extended to Dr. Martin Barone of GM R&D (now retired) for his valuable comments on this work at various times during its development.

References

[1] J.R. Brown, The lost foam casting process, Metals Mater. 8 (1992) 550–555.
[2] Q. Zhao, T.W. Gustafson, M. Hoover, M.C. Flemings, Fold formation in the lost foam aluminum process, in: S.K. Das (Ed.), Aluminum 2003, TMS, Warrendale, 2003, pp. 121–132.
[3] M.R. Barone, D.A. Caulk, A foam ablation model for lost foam casting of aluminum, Int. J. Heat Mass Transfer 48 (2005) 4132–4149.
[4] D.D. Goettsch, Unpublished research, 2000.
[5] X. Liu, C.W. Ramsay, D.R. Askeland, Study on mold filling control mechanisms in the EPC process, AFS Trans. 102 (1994) 903–914.
[6] Y. Sun, H.L. Tsai, D.R. Askeland, Investigation of wetting and wicking properties of refractory coating in the EPC process, AFS Trans. 100 (1992) 297–308.
[7] Q. Zhao, J.T. Burke, T.W. Gustafson, Foam removal mechanism in aluminum lost foam casting, AFS Trans. 110 (2002) 1399–1414.
[8] E.H. Niemann, Expandable polystyrene pattern material for the lost foam process, AFS Trans. 96 (1998) 793–798.
[9] S. Mehta, S. Biederman, S. Shivkumar, Thermal degradation of foamed polystyrene, J. Mater. Sci. 30 (1995) 2944–2949.
[10] C.H.E. Tseng, D.R. Askeland, Thermal and chemical analysis of the foam, refractory coating and sand in the EPC process, AFS Trans. 100 (1992) 509–518.
[11] J. Rossacci, S. Shivkumar, Influence of EPS bead fusion on pattern degradation and casting formation in the lost foam process, J. Mater. Sci. 38 (2003) 2321–2330.
[12] H.E. Littleton, T. Molibog, W. Sun, The role of pattern permeability in lost foam casting, AFS Trans. 111 (2003) 1265–1277.
[13] E.M. Sparrow, R.D. Cess, Radiation Heat Transfer, McGraw-Hill, New York, 1978, pp. 141–142.
[14] A.E. Scheidegger, The Physics of Flow Through Porous Media, third ed., University of Toronto Press, Toronto, 1974, p. 102.
[15] C.-H. Tseng, D.R. Askeland, A study of selected process parameters for the evaporative pattern casting process, AFS Trans. 99 (1991) 455–464.
[16] R.P. Walling, J.A. Dantzig, Mechanisms if mold filling in the EPC process, AFS Trans. 102 (1994) 849–854.
[17] M. Sands, S. Shivkumar, Influence of coating thickness and sand fineness on mold filling in the lost foam casting process, J. Mater. Sci. 38 (2003) 667–673.
[18] G.K. Batchelor, An Introduction to Fluid Dynamics, Cambridge University Press, New York, 1967, p. 237.
[19] S. Shivkumar, B. Gallois, Physico-chemical aspects of the full mold casting of aluminum alloys. Part I: The degradation of polystyrene, AFS Trans. 97 (1987) 791–800.